

Chiral bound states in a staggered array of coupled resonators

Wu-Lin Jin(金伍林), Jing Li(李静), Jing Lu(卢竞), Zhi-Rui Gong(龚志瑞), and Lan Zhou(周兰)

Citation: Chin. Phys. B, 2024, 33 (**2**): 020302. DOI: 10.1088/1674-1056/ad0bf0
Journal homepage: http://cpb.iphy.ac.cn; http://iopscience.iop.org/cpb

What follows is a list of articles you may be interested in

Wave function collapses and 1/*n* energy spectrum induced by a Coulomb potential in a one-dimensional flat band system

Yi-Cai Zhang(张义财)
Chin. Phys. B, 2022, 31 (**5**): 050311. DOI: 10.1088/1674-1056/ac3653

Exact solutions of the Schrödinger equation for a class of hyperbolic potential well

Xiao-Hua Wang(王晓华), Chang-Yuan Chen(陈昌远), Yuan You(尤源), Fa-Lin Lu(陆法林), Dong-Sheng Sun(孙东升), and Shi-Hai Dong(董世海)
Chin. Phys. B, 2022, 31 (**4**): 040301. DOI: 10.1088/1674-1056/ac3392

Geometric quantities of lower doubly excited bound states of helium

Chengdong Zhou(周成栋), Yuewu Yu(余岳武), Sanjiang Yang(杨三江), and Haoxue Qiao(乔豪学)
Chin. Phys. B, 2022, 31 (**3**): 030301. DOI: 10.1088/1674-1056/ac1b88

Efficient and stable wireless power transfer based on the non-Hermitian physics

Chao Zeng(曾超), Zhiwei Guo(郭志伟), Kejia Zhu(祝可嘉), Caifu Fan(范才富), Guo Li(李果), Jun Jiang(江俊), Yunhui Li(李云辉), Haitao Jiang(江海涛), Yaping Yang(羊亚平), Yong Sun(孙勇), and Hong Chen(陈鸿)
Chin. Phys. B, 2022, 31 (**1**): 010307. DOI: 10.1088/1674-1056/ac3815

Detection of spin current through a quantum dot with Majorana bound states

Ning Wang(王宁), Xingtao An(安兴涛), and Shuhui Lv(吕树慧)
Chin. Phys. B, 2021, 30 (**10**): 100302. DOI: 10.1088/1674-1056/abff1c

---

Chiral bound states in a staggered array of coupled resonators

Wu-Lin Jin(金伍林)[1], Jing Li(李静)[1], Jing Lu(卢竞)[1], Zhi-Rui Gong(龚志瑞)[2], and Lan Zhou(周兰)[1,†]

[1] *Synergetic Innovation Center for Quantum Effects and Applications, Key Laboratory for Matter Microstructure and Function of Hunan Province, Key Laboratory of Low-Dimensional Quantum Structures and Quantum Control of the Ministry of Education, Synergetic Innovation Center for Quantum Effects and Applications, Institute of Interdisciplinary Studies, Xiangjiang-Laboratory and Department of Physics, Hunan Normal University, Changsha* 410081, *China*

[2] *College of Physics and Optoelectronic Engineering, Shenzhen University, Shenzhen* 518060, *China*

(Received 18 August 2023; revised manuscript received 2 November 2023; accepted manuscript online 13 November 2023)

We study the chiral bound states in a coupled-resonator array with staggered hopping strengths, which interacts with a two-level small atom through a single coupling point or two adjacent ones. In addition to the two typical bound states found above and below the energy bands, this system presents an extraordinary chiral bound state located within the energy gap. We use the chirality to quantify the breaking of the mirror symmetry. We find that the chirality value undergoes continuous changes by tuning the coupling strengths. The preferred direction of the chirality is controlled not only by the competition between the intracell and the intercell hoppings in the coupled-resonator array, but also by the coherence between the two coupling points. In the case with one coupling point, the chirality values varies monotonously with difference between the intracell hopping and the intercell hoppings. While in the case with two coupling points, due to the coherence between the two coupling points the perfect chiral states can be obtained.

Keywords: bound states, two-level small atom, coupled-resonator array, chirality

PACS: 03.65.Pm, 03.65.–w **DOI:** 10.1088/1674-1056/ad0bf0

1. Introduction

Waveguide quantum electrodynamics (QED) studies the interaction of quantum emitters and photons propagating in a one-dimensional (1D) waveguide. The reduced dimensionality makes it possible for individual photons to be efficiently absorbed by even a single atom, which gives rise to strong correlations between photons.[1–3] A coupled-resonator array (CRA) is an arrangement of an infinite number of low-loss resonators with nearest-neighbor coupling, where photons move by direct hopping between the adjacent resonator. The CRA is an important 1D waveguide for studying waveguide QED due to its advantage of addressability of individual sites, high controllability, and the great degree of flexibility in their geometric design. The nontrivial modal dispersion relation of CRAs stimulates the investigation of photon transport which leads to many intriguing phenomena and application, such as single-photon switches,[4,5] super-cavities,[6,7] quantum routers,[8–10] and perfect mode conversion.[11]

One typical arrangement of CRAs is a quantum emitter coupling via Jaynes–Cummings-type interaction to only one resonator of the CRA with identical physical properties of resonators and uniform-hopping rates.[12–14] In the single-excitation sector, this single-atom CRA supports unbound stationary states with energies forming a cosine-shaped band, and two localized atom-photon bound states with energies slightly outside the continuum,[5,15] where each bound state is localized and symmetrical around the resonator coupling to the quantum emitter. The dynamics of the excitation in this single-atom CRA shows that the formation of atom–photon bound states results in the partial field localization and atomic population trapping.[16,17] The non-local coupling of the quantum emitter to the CRA with the cosine-shaped band has been studied,[18,19] bound states with energies outside the band are also been found.

In this work, we study a system in which a two-level small atom is coupled to adjacent resonators in a one-dimensional (1D) CRA with staggered hopping strengths (referring to a staggered CRA for short) via electric dipoles. It is different from the system of a two-level giant atom non-locally couples to two non-adjacent resonators in the Su–Schrieffer–Heeger (SSH) chain in Ref. [20]. More importantly, this system is simple to implement. In the absence of the two-level small atom, the staggered CRA forms two propagating bands with nonlinear dispersion without bound states, which is different from the system of a staggered CRA with finite length.[21–28] Those propagating bands are the complete basis of the Hilbert space of the photon which apparently possess the finite probability to appear at the large distance. When the two-level small atom is introduced, the bound state can be regarded as a linear combination of those propagating bands. In this sense, the localization of the photon around the two-level small atom is considered as the coherence creation of the propagating bands in the vicinity of the two-level small atom and the simultaneous coherence destruction of the propagating bands at large distance. Hence the bound states emerge in such system. It is natural to ask the following questions: How many bound states in a staggered CRA? Do they still have the reflection symmetry around the resonator that the two-level small atom

†Corresponding author. E-mail: zhoulan@hunnu.edu.cn

© 2024 Chinese Physical Society and IOP Publishing Ltd

is coupled to? If mirror symmetry is broken, how to measure and adjust this asymmetry? To find the answers to these questions, we study both local and non-local coupling of a two-level small atom to the staggered CRA. The local coupling means that the two-level small atom only interacts with one resonator. For non-local coupling, we only consider the two-level small atom only interacts with two adjacent resonators.

The paper is organized as follows. In Section 2, we propose the model describing the interaction between a staggered array of coupled resonators and a two-level small atom, and the equations of the probability amplitudes are presented in single-excitation subspace. In Section 3, we derive the condition for the single-photon bound states when two bands are presented, then introduce chirality to measure the mirror asymmetry of the bound states, achieve the control of the chirality of the bound states when the two-level small atom is locally or non-locally coupled to the staggered array and conduct an in-depth analysis of the directionality of chirality and the physical mechanisms. Finally, a summary has been made.

2. Model for a two-level small atom non-locally coupled to a staggered array

The model system we proposed is depicted schematically in Fig. 1. A 1D array of identical, single-mode resonators is coupled to an individual two-level small atom. Each resonator is modeled as a single harmonic oscillator mode of frequency ω. Nearest-neighbor resonators are coupled with staggered hopping energies where the two possible hopping energies $t+\delta$ and $t-\delta$ are interspersed along the array. The staggered CRA can be realized by circuit QED, that is, an array of coupled inductor–capacitor (LC) resonators is utilized to simulate the staggered CRA, and the coupling strength between LC resonators is controlled by capacitance and mutual inductance.[21,22] We cast the array into a tight-binding chain of equally-spaced sites with staggered hopping strength, which seems similar to the Peierls distorted chain, but the chain is assumed to be infinitely long in both direction. The free Hamiltonian of the staggered CRA reads

$$\hat{H}_0 = \sum_j \omega\left(\hat{a}_j^\dagger \hat{a}_j + \hat{b}_j^\dagger \hat{b}_j\right) - \sum_j (t+\delta)\left(\hat{a}_j^\dagger \hat{b}_j + \text{h.c.}\right) - \sum_j (t-\delta)\left(\hat{b}_{j-1}^\dagger \hat{a}_j + \text{h.c.}\right), \tag{1}$$

where the bosonic ladder operator $\hat{a}_j$ ($\hat{b}_j$) annihilate a photon at the a (b) resonator of the j-th unit cell marked by rectangles in Fig. 1. $t+\delta$ is the intracell hopping and $t-\delta$ is the intercell hopping. The first term in Eq. (1) is the on-site contribution, the other terms are responsible for the tunneling of photons between adjacent resonator. For $\delta = 0$, we retrieve the CRA with uniform hopping energy usually considered in the studies of single-photon transport.[5–9,12–14,16–19,29–32] The Fourier transform and some algebra reveal that the staggered CRA support Bloch bands and Bloch waves with the dispersion relation

$$\omega_k^{\pm} = \omega \pm \sqrt{2\left(t^2+\delta^2\right) + 2\left(t^2-\delta^2\right)\cos(kl)}, \tag{2}$$

where k is the momentum along the staggered CRA. The energy spectrum of the staggered CRA is two separate bands, the width of each band is $2(t-\delta)$ and the band gap is 4δ.

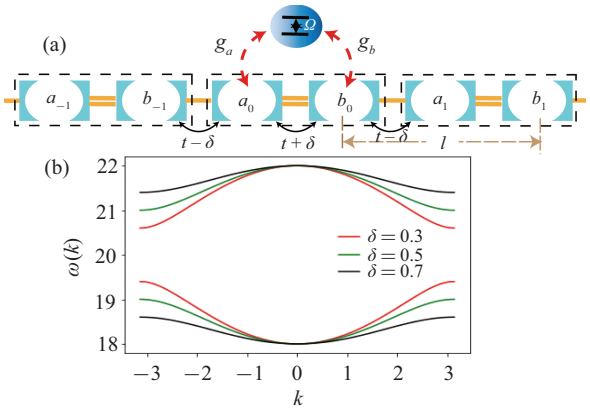


Fig. 1. (a) Schematic depiction of a two-level small atom non-local coupled to the nearest resonators in a staggered array made of coupled resonators. Dashed boxes indicate the unit cells. (b) The dispersion relation of the dimer chain for $\delta \neq 0$. All parameters are in units of the hop strength t.

The excited state $|e\rangle$ and ground state $|g\rangle$ of the two-level small atom are separated by the Bohr frequency Ω, and their transition is electric-dipole coupling to the mode of the adjacent resonators at the 0-th cell. Under the rotating-wave approximation the Hamiltonian of the bare two-level small atom and the transfer of excitations between the two-level small atom and field in the staggered CRA are described by

$$\hat{H}_1 = \Omega\,|e\rangle\langle e| + \left(g_a \hat{a}_0^\dagger + g_b \hat{b}_0^\dagger\right)\hat{\sigma}_- + \text{h.c.}, \tag{3}$$

where σ_z is the z component of the Pauli matrices which acts on the two internal states $|e\rangle$ and $|g\rangle$ and σ_- (σ_+) is its corresponding lowering (raising) operator. The non-local coupling between the two-level small atom and the staggered CRA can be realized by capacitors, and the coupling strengths can be adjusted by capacitors.[34]

The operator $\hat{N} = \sum_j (\hat{a}_j^\dagger \hat{a}_j + \hat{b}_j^\dagger \hat{b}_j) + |e\rangle\langle e|$ commutes with the total Hamiltonian $H = H_0 + H_1$ of the system, which features a fixed number of excitations. The eigenstates of the Hamiltonian H can be constructed by the eigenstates of the conserved quantity $\hat{N}$ with the ansatz

$$|\varepsilon\rangle = \left(\sum_j \alpha_j \hat{a}_j^\dagger + \sum_j \beta_j \hat{b}_j^\dagger + u_e \hat{\sigma}_+\right)|\emptyset\rangle, \tag{4}$$

where $\hat{a}_j^\dagger|\emptyset\rangle$ ($\hat{b}_j^\dagger|\emptyset\rangle$) denotes a single photon occupying the mode of the a (b) resonator at the j-th unit cell, and $\hat{\sigma}_+|\emptyset\rangle$ stands for the two-level small atom excited state. Substituting the ansatz in stationary Schrödinger equation leads to a set of relations for the coefficients α_j and β_j

$$\varepsilon\alpha_j = \omega\alpha_j - (t+\delta)\beta_j - (t-\delta)\beta_{j-1} + g_a u_e \delta_{j,0},$$

$$\varepsilon\beta_j = \omega\beta_j - (t+\delta)\,\alpha_j - (t-\delta)\,\alpha_{j+1} + g_b u_e \delta_{j,0},$$
$$\varepsilon u_e = \Omega u_e + g_a\alpha_0 + g_b\beta_0. \tag{5}$$

By removing the amplitude u_e, the equations for the amplitudes reduce to

$$\begin{aligned}(\varepsilon-\omega)\,\alpha_j &= (\delta-t)\,\beta_{j-1} - (t+\delta)\,\beta_j \\ &\quad + \delta_{j,0}\,(V_a\alpha_0 + G\beta_0),\\ (\varepsilon-\omega)\,\beta_j &= (\delta-t)\,\alpha_{j+1} - (t+\delta)\,\alpha_j \\ &\quad + \delta_{j,0}\,(G\alpha_0 + V_b\beta_0),\end{aligned} \tag{6}$$

where we have defined local energy-dependent deltalike potentials

$$V_n = \frac{g_n^* g_n}{\varepsilon-\Omega},\quad n=a,b \tag{7}$$

and the effective dispersive coupling strength

$$G = \frac{g_a^* g_b}{\varepsilon-\Omega}. \tag{8}$$

When one of the coupling strength $g_n = 0$, we retrieve the model where the two-level small atom interacts with only one resonator of the staggered array, i.e., the two-level small atom is locally coupled to the staggered array.

3. Single-photon bound states

In the absence of the two-level small atom, the staggered CRA exhibits two continuous spectrums of propagating waves. The presence of the two-level small atom breaks down the translation symmetry of the staggered array, so the nonpropagating eigenstates are formed, which are called the bound states (BSs). The bound states are dressed atom-field eigenstates localized around the quantum emitter.[5,6,8,9,17,19,32] In Fig. 2, we plot the eigen-energy in the single excitation subspace by numerically diagonalising the Hamiltonian in the real space. In general, it can be found that there are three bound states: one lies above all bands (called BS I), one lies within the band gap (called BS II), and one lies below all bands (called BS III). Nevertheless, when $g_a = g_b = g$ the number of bound states can be controlled by adjusting g and δ, so that there is one, two or three bound states.

Since bound states are waves that remain localized, we assume the following solutions to Eq. (6) with $k_0 = 0, \pi$

$$\begin{aligned}\alpha_j &= \begin{cases} A_{\rm L}^{\kappa}\,\mathrm{e}^{\mathrm{i}k_0 jl + \kappa jl}\,\Theta(-j), \\ A_{\rm R}^{\kappa}\,\mathrm{e}^{\mathrm{i}k_0 jl - \kappa jl}\,\Theta(j), \end{cases}\\ \beta_j &= \begin{cases} B_L^{\kappa}\,\mathrm{e}^{\mathrm{i}k_0 jl - \kappa(|j|-1/2)l}\,\Theta(-j), \\ B_R^{\kappa}\,\mathrm{e}^{-\kappa l}\,\mathrm{e}^{\mathrm{i}k_0 jl - \kappa(|j|-1/2)l}\,\Theta(j), \end{cases}\end{aligned} \tag{9}$$

which decay exponentially with the distance from the site that the two-level small atom is coupled to, where $\Theta(j) = 1$ for $j > 0$ and $\Theta(j) = 0$ for $j < 0$. The relation of the imaginary wave vector $\kappa > 0$ and the energy of a localized photon outside of the bands is obtained as

$$\varepsilon = \omega \pm \sqrt{2(t^2+\delta^2) + (t^2-\delta^2)\left(\mathrm{e}^{-\mathrm{i}k_0 l + \kappa l} + \mathrm{e}^{\mathrm{i}k_0 l - \kappa l}\right)} \tag{10}$$

by considering the region far away from the two-level small atom, so do the following ratios:

$$\begin{aligned}\frac{B_{\rm L}^{\kappa}}{A_{\rm L}^{\kappa}} &= \frac{(t+\delta)\,\mathrm{e}^{-\kappa(l/2)} + (t-\delta)\,\mathrm{e}^{\mathrm{i}k_0 l + \kappa(l/2)}}{\omega-\varepsilon},\\ \frac{B_{\rm R}^{\kappa}}{A_{\rm R}^{\kappa}} &= \frac{\omega-\varepsilon}{(t+\delta)\,\mathrm{e}^{-\kappa(l/2)} + (t-\delta)\,\mathrm{e}^{-\mathrm{i}k_0 l + \kappa(l/2)}},\end{aligned} \tag{11}$$

which indicates that

$$\frac{B_{\rm L}^{\kappa}}{A_{\rm L}^{\kappa}} = \frac{A_{\rm R}^{\kappa}}{B_{\rm R}^{\kappa}}. \tag{12}$$

For $k_0 = 0$, equation (10) gives the energy

$$\varepsilon_0^{\pm} = \omega \pm \sqrt{2(t^2+\delta^2) + 2(t^2-\delta^2)\cosh(kl)}$$

lying above or below two bands. For $k_0 = \pi$, equation (10) shows that the energy

$$\varepsilon_\pi^{\pm} = \omega \pm \sqrt{2(t^2+\delta^2) - 2(t^2-\delta^2)\cosh(kl)}$$

is inside the band gap.

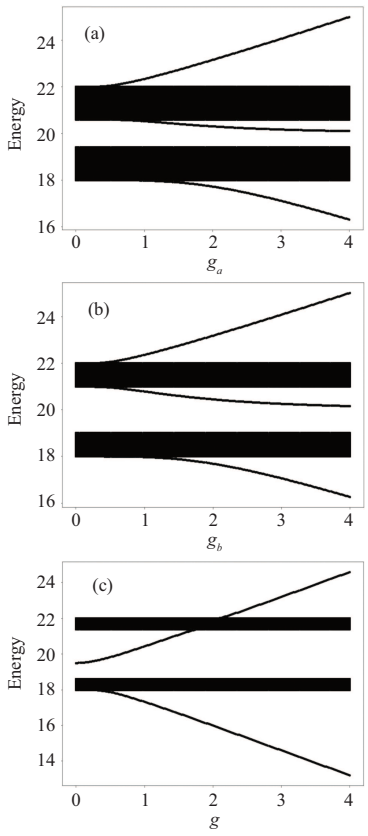


Fig. 2. The spectrum as a function of the coupling strength with $\omega = 20$. (a) $\Omega = 21.5$, $\delta = 0.3$, $g_b = 0$; (b) $\Omega = 21.5$, $\delta = 0.5$, $g_a = 0$; (c) $\Omega = 19.5$, $\delta = 0.7$, $g_a = g_b = g$. All parameters are in units of the hop strength t.

Applying Eqs. (9) and (11) to the discrete scattering equation (6) at $j=\pm1$, the amplitudes for the $j=0$ cell read

$$\alpha_0 = A_{\rm L}^{\kappa}, \quad \beta_0 = B_{\rm R}^{\kappa}\,{\rm e}^{-\kappa(l/2)}. \tag{13}$$

By substituting Eq. (13) and spatial exponential-decay solution (9) to Eqs. (6) at $j=0$, we achieve the condition for the existence of the bound state

$$\begin{aligned}(t+\delta-G)^2 = &\left[\varepsilon-\omega-V_a+(t-\delta)\frac{B_{\rm L}^{\kappa}}{A_{\rm L}^{\kappa}}{\rm e}^{-{\rm i}k_0 l-\kappa(l/2)}\right]\\ &\times\left[\varepsilon-\omega-V_b+(t-\delta)\frac{A_{\rm R}^{\kappa}}{B_{\rm R}^{\kappa}}{\rm e}^{{\rm i}k_0 l-\kappa(l/2)}\right]\end{aligned} \tag{14}$$

as well as the following ratio:

$$\frac{A_{\rm L}^{\kappa}}{A_{\rm R}^{\kappa}} = \frac{t+\delta}{t+\delta-G} - V_b\frac{t+\delta+(t-\delta)\,{\rm e}^{{\rm i}k_0 l-\kappa l}}{(\varepsilon-\omega)(t+\delta-G)}, \tag{15a}$$

$$\frac{B_{\rm R}^{\kappa}}{B_{\rm L}^{\kappa}} = \frac{(t+\delta)\,{\rm e}^{\kappa l}}{t+\delta-G} - V_a\frac{(t+\delta)\,{\rm e}^{\kappa l}+(t-\delta)\,{\rm e}^{-{\rm i}k_0 l}}{(\varepsilon-\omega)(t+\delta-G)}. \tag{15b}$$

The number of the bound states completely determined by the above conditions.

3.1. Local coupling

The local coupling of the two-level small atom to the staggered CRA corresponds to the case with either $g_a=0$ or $g_b=0$, which means the effective dispersive coupling strength $G=0$. When one fold the system around the line perpendicular to the array and passing the site that the two-level small atom is coupled to, the left half of the line is not the exact reflection of its other half as long as $\delta\neq0$. This property leads to the mirror asymmetry of the bound state which is characterized by $A_{\rm L}^{\kappa}\neq A_{\rm R}^{\kappa}$ or $B_{\rm L}^{\kappa}\neq B_{\rm R}^{\kappa}\,{\rm e}^{-\kappa l}$ in Eq. (9). When $g_b=0$, the two-level small atom is coupled to the a_0 resonator, whose site is the location of the line of the symmetry. Equation (15) indicates that amplitude $A_{\rm L}^{\kappa}=A_{\rm R}^{\kappa}$, which means the asymmetry is characterized by the amplitudes of the b resonators. When $g_a=0$, the two-level small atom is coupled to the b_0 resonator, the line of symmetry is located at coordinate $l/2$. One can find that $B_{\rm L}^{\kappa}=B_{\rm R}^{\kappa}\,{\rm e}^{-\kappa l}$ from Eq. (15), so the asymmetry is completely characterized by the amplitudes of the a resonators. The above results are consistent with results in Ref. [33].

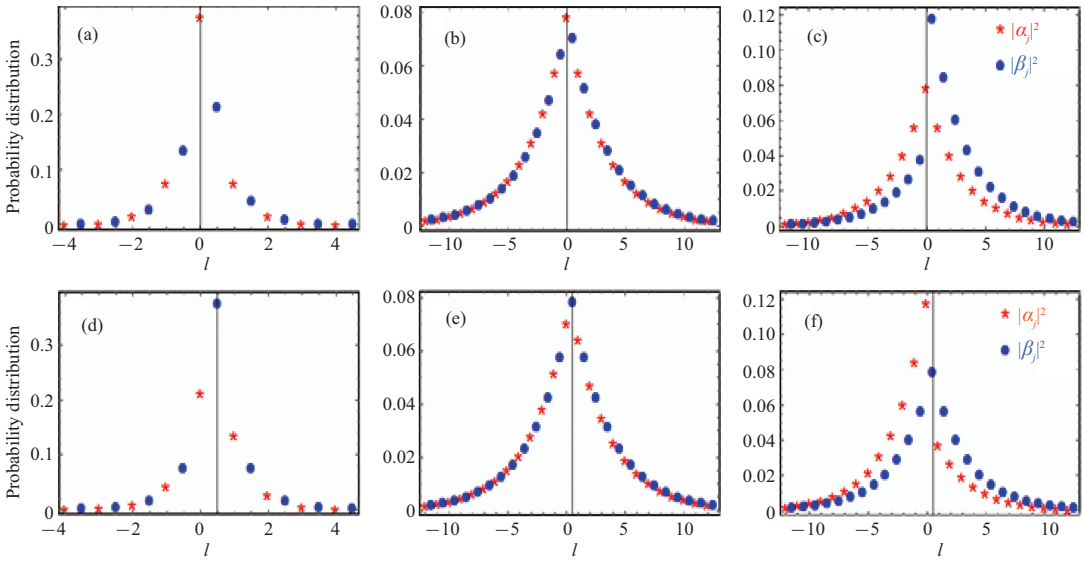


Fig. 3. The probability distribution of the bound state I (panels (a) and (d)), III (panels (b) and (e)), and II (panels (c) and (f)). The two-level small atom is coupled only to the a_0 resonator in the upper panels (panels (a)–(c)). The two-level small atom is coupled only to the b_0 resonator in lower panels (panels (d)–(f)). All parameters are in units of the hop strength t and $\omega=20$, $\Omega=21.5$, $\delta=0.3$.

In Fig. 3, we have plotted the probability distribution of the bound state I (panels (a) and (d)), III (panels (b) and (e)), and II (panels (c) and (f)) when $g_a=0.7$, $g_b=0$ (panels (a)–(c)) or $g_a=0$, $g_b=0.7$ (panels (d)–(f)) respectively. The black line located at origin in each upper panel and coordinate $l/2$ in each lower panel is the line of symmetry. It can be observed that: (i) The red stars (blue dots) distribute symmetrically around the black line in each upper (lower) panel. (ii) All the bound states prefer to localize at the right side of the two-level small atom for $g_b=0$, and *vice versa* for $g_a=0$. (iii) Panels (d), (e), and (f) appear as the reflection of the panels (a), (b), and (c) followed by a shift to the right by $l/2$ distance, respectively. So in the following, we focus our discussion on the case with $g_b=0$.

To further quantify the mirror symmetry of bound states, we introduce the chirality[34]

$$S = \frac{s_{\rm L}-s_{\rm R}}{s_{\rm L}+s_{\rm R}} \tag{16}$$

to depict the asymmetry of the bound state in the left-side and right-side of the symmetry line at the origin

$$s_{\rm L} = \sum_{j=-\infty}^{-1}|\beta_j|^2, \tag{17a}$$

$$s_{\rm R} = \sum_{j=1}^{\infty}|\beta_j|^2+|\beta_0|^2, \tag{17b}$$

where $S>0$ ($S<0$) indicates that the chirality prefers the left (right) direction, and $S\to 1$ ($S\to -1$) corresponds to perfect left (right) chirality. The chirality can be further expressed as

$$S=\frac{1-\left|B_{\mathrm{R}}^{\kappa}/B_{\mathrm{L}}^{\kappa}\right|^{2}}{1+\left|B_{\mathrm{R}}^{\kappa}/B_{\mathrm{L}}^{\kappa}\right|^{2}} \tag{18}$$

with the help of wave function in Eq. (9). To present how to tune the chirality of these bound states, we plot the chirality S as a function of δ in Fig. 4 with different Bohr frequency Ω for fixed coupling strength.

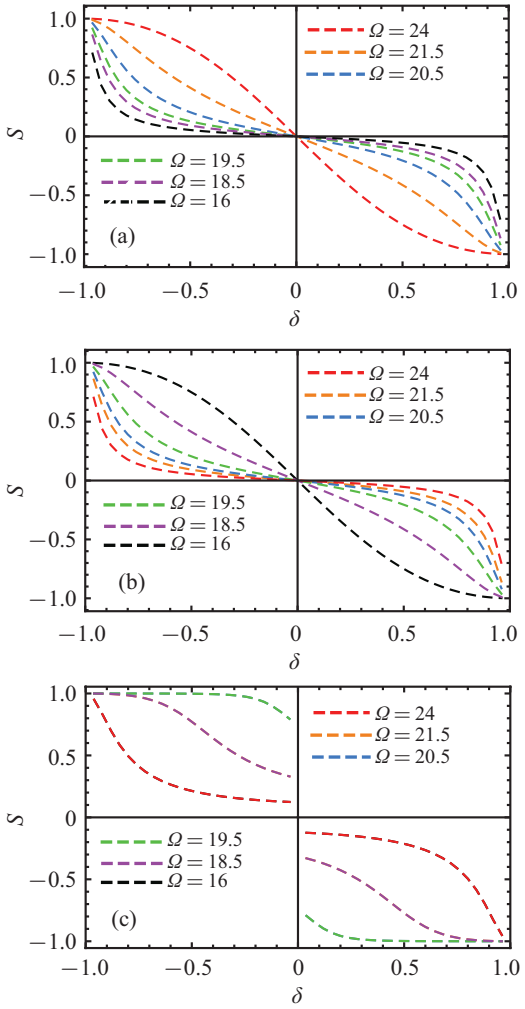


Fig. 4. The chirality of the bound state I (a), III (b), and II (c) versus δ for local coupling. Here, $\omega=20$, $g_a=0.7$. All parameters are in units of the hop strength t.

It can be found that (i) one can continuously tune the chirality of bound states I and III over the whole range $\delta\in[-1,1]$, so does the chirality of bound state II as long as the hopping strengths are staggered. In particular, when $\delta\to 0$, the chirality of bound states I and III tends to 0, however the chirality of bound state II is far from 0. Without the staggering, i.e., $\delta=0$ the staggered array becomes a uniform array, and bound state II disappears. The chirality of bound state II is discontinuous at $(0^{-},0^{+})$, which corresponds to the closure and opening of the band of the staggered CRA, and also to the different topology of the staggered CRA for positive or negative δ. (ii) The chirality prefers left direction when $\delta<0$ and prefers right direction when $\delta>0$, i.e., the photon would like to appear at the left side of the line of the symmetry when $\delta<0$ and at the right side when $\delta>0$. The underlying mechanism is the following: the two-level small atom creates a single photon into the mode of the a_0 resonator, from where the photon can hop to other resonator. Single photon hop to the side where the hopping strength is larger, hence, the hopping strength determines the chiral. The discontinunity of the chirality of the bound state II actually relates to the topology of the staggered CRA, where $\delta<0$ and $\delta>0$ corresponds to opposite widing number. (iii) The left (right) chirality increases as Ω increases for bound state I and decreases as Ω increases for bound state III. However, the chirality of the bound state II increases as the Bohr frequency Ω is closer to the resonator's frequency ω. When $\delta=\pm 1$, the staggered CRA falls apart to a sequence of disconnected dimers. The energy of the dimer which couples to the two-level small atom is different from the energies $\omega\pm 2t$ of other dimers, whose eigenstates are the even and odd superpositions of the two sites forming a dimer. A single photon is completely localized at the dimer the two-level small atom is coupled. Hence, the chirality is completely determined by the site which is close to the a_0 resonator, i.e., the amplitude β_0 or β_{-1}.

3.2. Non-local coupling

We now consider the case that all coupling strength $g_n\neq 0$. We assume that the two-level small atom is located at the middle of the unit cell at $j=0$, so, the line of symmetry is located at coordinate $l/4$. The probabilities at the right and left side of the line become

$$S_{\mathrm{L}}=\sum_{j=-\infty}^{-1}\left(\left|\alpha_j\right|^2+\left|\beta_j\right|^2\right)+\left|\alpha_0\right|^2, \tag{19a}$$

$$S_{\mathrm{R}}=\sum_{j=1}^{\infty}\left(\left|\alpha_j\right|^2+\left|\beta_j\right|^2\right)+\left|\beta_0\right|^2, \tag{19b}$$

and the chirality of bound states reads

$$S=\frac{\left|A_{\mathrm{L}}^{\kappa}\right|^2\mathrm{e}^{\kappa l}-\left|A_{\mathrm{R}}^{\kappa}\right|^2\mathrm{e}^{-\kappa l}+\left|B_{\mathrm{L}}^{\kappa}\right|^2-\left|B_{\mathrm{R}}^{\kappa}\right|^2}{\left|A_{\mathrm{L}}^{\kappa}\right|^2\mathrm{e}^{\kappa l}+\left|A_{\mathrm{R}}^{\kappa}\right|^2\mathrm{e}^{-\kappa l}+\left|B_{\mathrm{L}}^{\kappa}\right|^2+\left|B_{\mathrm{R}}^{\kappa}\right|^2}. \tag{20}$$

We firstly discuss the chirality of the bound states when $g_a=g_b$. In this case, equation (15) becomes

$$\frac{A_{\mathrm{L}}^{\kappa}}{A_{\mathrm{R}}^{\kappa}}=\frac{B_{\mathrm{R}}^{\kappa}}{B_{\mathrm{L}}^{\kappa}}\mathrm{e}^{-\kappa l}. \tag{21}$$

With the help of Eq. (12), we obtain $S=0$, which can be understood easily because the system has mirror symmetry around the line passing through coordinate $l/4$. This result told us that chirality may arise when $g_a\neq g_b$. In Fig. 5, we plot the chirality S of the bound state versus δ.

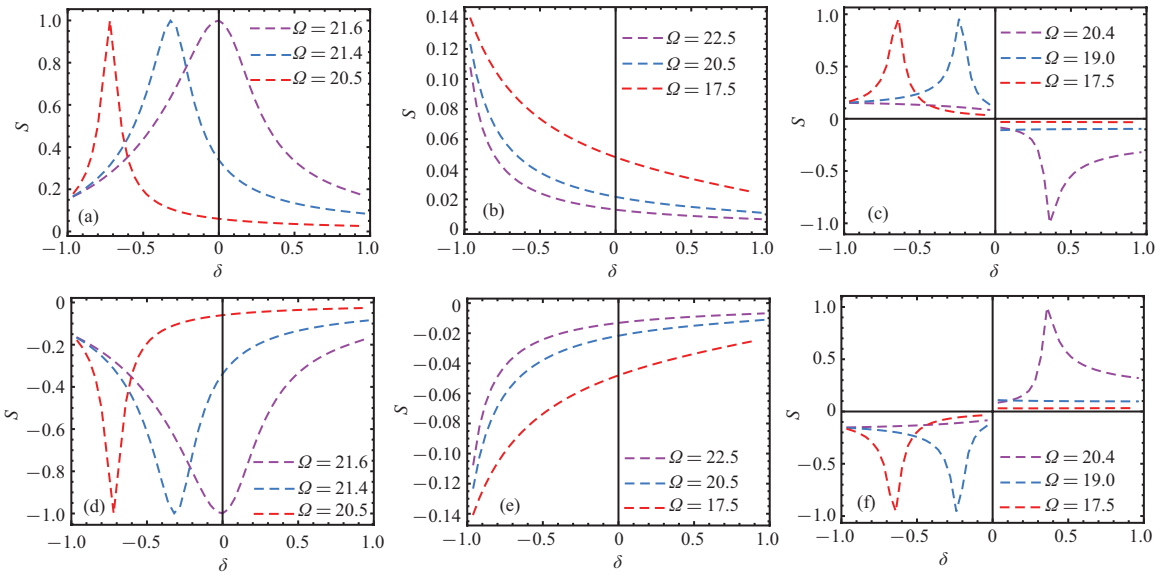


Fig. 5. The chirality of the bound state I (panels (a) and (d)), III (panels (b) and (e)), and II (panels (c) and (f)) versus δ for non-local coupling. Here, $g_a = 0.7$, $g_b = 0.6$ for upper panels and $g_a = 0.6$, $g_b = 0.7$ for lower panels. All parameters are in units of the hop strength t and $\omega = 20$.

It can be observed that the chirality of bound states I and III are determined by the coupling strength, i.e., the chirality of bound states I and III prefers the left direction when $g_a > g_b$ and *vice versa* when $g_a < g_b$. One can continuously tune the chirality of bound states I and III over the whole range $\delta \in [-1, 1]$, so does the chirality of bound states II as long as the hopping strengths are staggered. Specially, the chirality of bound state II can change its direction as δ varies from negative to positive. The chirality of bound state III only varies monotonously with δ, and decreases as Ω increases. However, the perfect chirality can be achieved for the bound states I and II, and the perfect chirality shifts to the right as Ω increases. Actually, each lower panel in Fig. 5 can be obtained by turning the corresponding upper panel 180° about the horizontal axis. Hereafter, we will focus on the case with $g_a > g_b$.

To understand why the chirality prefers the same direction for bound states I and III no matter how δ change and why bound state II changes its chirality as δ changes, we consider the fully dimerized limits characterized by $\delta = \pm t$. Most dimers yield energies $\omega \pm 2t$, the energy other than $\omega \pm 2t$ are formed by the dimer connected to the two-level small atom. Discussions can be restricted to the dimers that interact with the two-level small atom, as shown in Fig. 6. When $\delta = -t$, four resonators are involved (see Fig. 6(a)), the two-level small atom would like to emit the excitation to its left side rather than its right side. So all bound states prefer the left direction. When $\delta = t$, only two resonators are involved (see Fig. 6(b)). Although the two-level small atom would like to emit the excitation to the a_0 resonator, it can hop to the b_0 resonator easily. So the preferred direction of the bound states is decided by whether the ratio $|\beta_0/\alpha_0|^2$ larger or smaller than one,

$$1 - \frac{|\beta_0|^2}{|\alpha_0|^2} = \frac{g_a^2 - g_b^2}{(\varepsilon - \omega)(\varepsilon - \Omega) - g_b^2}. \tag{22}$$

Here, ε is the eigenenergy of the two-level small atom and the dimer at the $j = 0$ cell, it can take three values, ε_u, ε_l and ε_m, where ε_u is larger than $\omega + 2t$, ε_l is smaller than $\omega - 2t$ and ε_m is within the regime $(\omega - 2t, \omega + 2t)$. The poles E_1 and E_2 of Eq. (22) are the eigenergies in the absence of a_0 resonator with $E_1 > E_2$.

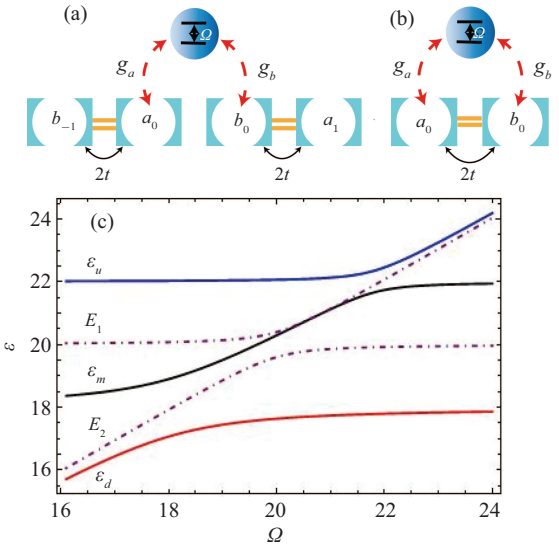


Fig. 6. Sketch of the system under study when (a) $\delta = -t$ and (b) $\delta = t$, and (c) the eigenenergy of the two-level small atom and the dimer and the poles E_1 and E_2 of Eq. (22) as a function of the Ω, where $\omega = 20$, $g_a = 0.9$, $g_b = 0.4$, $\delta = 1$.

In Fig. 6(b), we plot the eigenergies ε and E_i as a function of the Ω. It can be seen that $\varepsilon_u > E_1$, $\varepsilon_l < E_2$, and $E_1 > \varepsilon_m > E_2$, which indicates that the chirality of bound state II is different from that of bound states I and III, i.e., the chirality prefers the right direction for bound state II. The staggered coupled-resonator array is exactly described by the SSH model in Ref. [20], and the winding number of the SSH model changes from +1 for $\delta > 0$ to −1 for $\delta < 0$ discontinuously.

This is the nature of the discontinunity of the chirality of the bound state II. If $\delta = 0$, there is no topological properties of the uniformed coupled-resonator array and thus the state II also disappear.

4. Conclusion

For an array of resonators mutually interacted with staggered hopping strengths, we consider its interaction with a two-level small atom by a coupling point or two coupling points. Its single-photon spectrum has been studied and it is found that this system has two energy bands and three discrete spectra with one lying upper the bands and one lying below the bands, and another inside the band gap. The stationary states of the discrete spectra are analytically presented and are chiral bound states when coupling strengths have different magnitudes. One can tune the chirality of bound state II over the range $\delta \in [-t,0)\cup(0,t]$, and continuously tune the chirality of bound states I and III over the whole range $\delta \in [-t,t]$. In the case with one coupling point, the preferred direction of the chirality is controlled by the competition between the intracell hopping and the intercell hopping. In the case with two coupling points, the competition between two coupling strengths adjusts the chirality of all bound states, in addition, the chirality of bound state II change its direction as δ varies its sign for fixed coupling strengths. Due to the discontinunity of the chirality of the bound state II inheriting from the topology of the CRA, the chirality can be tuned greatly by only slightly change the magnitude of δ. In Ref. [20], the authors proposed a tunable chiral bound states whose chirality is controllable. The coupling direction and strength between the adjacent superconductor qubits are totally controllable because they depend on the overlap of the tunable chiral bound states, which may facilitate the construction of the large scale quantum network.

Acknowledgements

Project supported by the National Natural Science Foundation of China (Grant Nos. 11975095, 12075082, 11935006, and 12247105), the Major Sci-Tech Program of Hunan Province, China (Grant No. 2023ZJ1010), and the Natural Science Foundation of Guangdong Province, China (Grant Nos. 2019A1515011400 and 2023A151501223).

References

[1] Shen J T and Fan S 2007 *Phys. Rev. Lett.* **98** 153003
[2] Zheng H X, Gauthier D J and Baranger H U 2010 *Phys. Rev. A* **82** 063816
[3] Shi T, Fan S H and Sun C P 2011 *Phys. Rev. A* **84** 063803
[4] Zhou L, Gong Z R, Liu Y X, Sun C P and Nori F 2008 *Phys. Rev. Lett.* **101** 100501
[5] Zhou L, Yang S, Liu Y X, Sun C P and Nori F 2009 *Phys. Rev. A* **80** 062109
[6] Zhou L, Dong H, Liu Y X, Sun C P and Nori F 2008 *Phys. Rev. A* **78** 063827
[7] Gong Z R, Ian H, Zhou L and Sun C P 2008 *Phys. Rev. A* **78** 053806
[8] Zhou L, Yang L P, Li Y and Sun C P 2013 *Phys. Rev. Lett.* **111** 103604
[9] Lu J, Zhou L, Kuang L M and Nori F 2014 *Phys. Rev. A* **89** 013805
[10] Ahumada M, Orellana P A, Domínguez-Adame F and Malyshev A V 2019 *Phys. Rev. A* **99** 033827
[11] Xu H S and Jin L 2022 *Phys. Rev. Res.* **4** L032015
[12] Wang Z H, Zhou L, Li Y and Sun C P 2014 *Phys. Rev. A* **89** 053813
[13] Yan W B and Fan H 2014 *Phys. Rev. A* **90** 053807
[14] Longo P, Schmitteckert P and Busch K 2010 *Phys. Rev. Lett.* **104** 023602
[15] Ahumada M, Orellana P A and Retamal J C 2018 *Phys. Rev. A* **98** 023827
[16] Lombardo F, Ciccarello F and Palma G M 2014 *Phys. Rev. A* **89** 053826
[17] Sánchez-Burillo E, Zueco D, Martín-Moreno L and García-Ripoll J J 2017 *Phys. Rev. A* **96** 023831
[18] Zhou L, Chang Y, Dong H, Kuang L M and Sun C P 2012 *Phys. Rev. A* **85** 013806
[19] Zhao W and Wang Z H 2020 *Phys. Rev. A* **101** 053855
[20] Cheng W J, Wang Z H and Liu Y X 2022 *Phys. Rev. A* **106** 033522
[21] Kim E J, Zhang X Y, Ferreira V S, Jash B, Iverson J K, Sipahigil A, Bello M, González-Tudela A, Mirhosseini M and Painter O 2021 *Phys. Rev. X* **11** 011015
[22] Liu Y B and Houck A A 2016 *Nat. Phys.* **13** 48
[23] Vega C, Bello M, Porras D and González-Tudela A 2021 *Phys. Rev. A* **104** 053522
[24] Asbóth J K, Oroszlány L and Pályi A 2016 *Lecture Notes in Physics* **919** pp. 1-9
[25] Ciccarello F 2011 *Phys. Rev. A* **83** 043802
[26] Almeida G M A, Ciccarello F, Apollaro T J G and Souza A M C 2016 *Phys. Rev. A* **93** 032310
[27] Scigliuzzo M, Calajó G, Ciccarello F, Lozano D P, Bengtsson A, Scarlino P, Wallraff A, Chang D, Delsing P and Gasparinetti S 2022 *Phys. Rev. X* **12** 031036
[28] Gao B, Li J, Jiang H W, Wang J S, Zhu C J, Xu J Q and Yang Y P 2021 *Opt. Express* **29** 31010
[29] Fong P T and Law C K 2017 *Phys. Rev. A* **96** 023842
[30] Xu X W, Chen A X, Li Y and Liu Y X 2017 *Phys. Rev. A* **95** 063808
[31] Wang Z H, Du L, Li Y and Liu Y X 2019 *Phys. Rev. A* **100** 053809
[32] Qiao L and Sun C P 2019 *Phys. Rev. A* **100** 063806
[33] Bello M, Platpro G, Cirac J I and Gonzalez-tudela A 2019 *Sci. Adv.* **5** eaaw0297
[34] Wang X, Liu T, Kockum A F, Li H R and Nori F 2021 *Phys. Rev. Lett.* **126** 043602